Pressure-Induced Fusogenic Conformation of Vesicular Stomatitis Virus Glycoprotein†

Andre M. O. Gomes,‡ Anderson S. Pinheiro,‡ Carlos F. S. Bonafe,§ and Jerson L. Silva*,‡

Programa de Biologia Estrutural, Departamento de Bioquímica Médica, Instituto de Ciências Biomédicas, Centro Nacional de Ressonância Magnética Nuclear de Macromoléculas, Universidade Federal do Rio de Janeiro, 21941-590 Rio de Janeiro, RJ, Brazil, and Departamento de Bioquímica, Instituto de Biologia, Universidade Estadual de Campinas, 13084-100, Campinas, SP, Brazil

Received November 20, 2002; Revised Manuscript Received March 13, 2003

ABSTRACT: Vesicular stomatitis virus (VSV) is composed of a ribonucleoprotein core surrounded by a lipid envelope presenting an integral glycoprotein (G). The homotrimeric VSV G protein exhibits a membrane fusion activity that can be elicited by low pH. The fusion event is crucial to entry into the cell and disassembly followed by viral replication. To understand the conformational changes involved in this process, the effects of high hydrostatic pressure and urea on VSV particles and isolated G protein were investigated. With pressures up to 3.0 kbar VSV particles were converted into the fusogenic conformation, as measured by a fusion assay and by the binding of bis-ANS. The magnitude of the changes was similar to that promoted by lowering the pH. To further understand the relationship between stability and conversion into the fusion-active states, the stability of the G protein was tested against urea and high pressure. High urea produced a large red shift in the tryptophan fluorescence of G protein whereas pressure promoted a smaller change. Pressure induced equal fluorescence changes in isolated G protein and virions, indicating that virus inactivation induced by pressure is due to changes in the G protein. Fluorescence microscopy showed that pressurized particles were capable of fusing with the cell membrane without causing infection. We propose that pressure elicits a conformational change in the G protein, which maintains the fusion properties but suppresses the entry of the virus by endocytosis. Binding of bis-ANS indicates the presence of hydrophobic cavities in the G protein. Pressure also caused an increase in light scattering of VSV G protein, reinforcing the hypothesis that high pressure elicits the fusogenic activity of VSV G protein. This "fusion-intermediate state" induced by pressure has minor changes in secondary structure and is likely the cause of nonproductive infections.

A virus particle is composed of either a membrane enveloped or a nonenveloped protein shell and nucleic acid. Enveloped animal viruses must undergo membrane fusion to deliver their genome into the host cell (*1*, *2*). Membrane fusion is crucial in many other biological functions such as trafficking of endocytic and exocytic vesicles within eukaryotic cells (*1*−*4*). In enveloped viruses, fusion is mediated by virus surface glycoproteins. The fusion event has been widely studied for several viruses including the myxoviruses, Ebola virus, influenza and parainfluenza viruses, filoviruses, and retroviruses (*4*). The most common feature of all of these viruses is that their fusion glycoproteins are synthesized as precursors that gain the function of membrane fusion by proteolytic cleavage (*3*, *5*). Vesicular stomatitis virus (VSV) belongs to a distinct group in which there is no postassembly proteolytic processing of the glycoprotein. Entry of VSV into cells occurs after endocytosis within the low-pH environment of the endosomes (*5*, *6*). Binding and fusion are mediated by VSV glycoprotein (G) (*6*−*9*). The VSV fusion process involves a series of steps that is initiated by exposure to low pH (*10*) and results in a conformational change in the G protein, which leads into the exposure of hydrophobic domains (*7*, *9*).

VSV is the prototype of the *Rhabdoviridae* and is composed of an RNA genome of negative sense, five viral proteins, and membrane lipids derived from the host cell (*11*). After entry, VSV interferes with several metabolic functions in the host cell. The infectious component of VSV is the ribonucleoprotein core, where the RNA is tightly encased by the nucleocapsid protein (N), also associated with two minor proteins: L and NS. The VSV membrane contains two proteins: an integral glycoprotein (G) and a peripheral matrix protein (M) that aligns in the inner surface of the virion membrane (*11*). Infection by VSV rapidly shuts off cellular RNA synthesis (*12*), as well as host-cell DNA replication and protein synthesis (*13*). We have previously shown that VSV G protein labeled with fluorescein isothiocyanate (FITC) appears initially in endocytic vesicles and rapidly migrates to the nucleus of infected cells (*14*).

† This work was supported in part by an international grant from the Howard Hughes Medical Institute to J.L.S. and by grants from Conselho Nacional de Desenvolvimento Científico e Tecnológico (CNPq), Programa de Núcleos de Excelência (PRONEX), and Fundação de Amparo à Pesquisa no Estado do Rio de Janeiro (FAPERJ) of Brazil to J.L.S.

* To whom correspondence should be addressed. Phone: 55-212562-6756. Fax: 55-212270-8647. E-mail: jerson@bioqmed.ufrj.br.

‡ Universidade Federal do Rio de Janeiro.

§ Universidade Estadual de Campinas.

10.1021/bi027207k CCC: $25.00
Published on Web 04/15/2003

Hydrostatic pressure has been used to study assembly of multimeric proteins and viruses (*15*−*17*). The combination of thermodynamic and structural approaches has shed light into the general rules that govern virus assembly (*18*−*21*). In several animal viruses, pressure induces inactivation with no change or even increase in the immunogenicity, suggesting pressure as an alternative method to produce vaccines (*22*−*25*). We have recently demonstrated that high pressure inactivates two membrane-enveloped viruses, influenza and Sindbis, by trapping the particles in a fusion intermediate state (*26*).

Here, we show that high pressure triggers a conformational change in the G protein, which makes the particle primed for fusion. Because pressure is a mild perturbation when compared with denaturants and high temperature, it elicits no dramatic changes in the structure of the whole particle. Nevertheless, the pressurized particles are not infectious. Different from other viruses the transition to the fusogenic conformation induced by pH in VSV is not irreversible. However, the increase in light scattering of VSV G protein and the changes in the binding of a hydrophobic probe (bis-ANS) produced by pressure were irreversible. This "fusion-active state" induced by pressure has minor changes in secondary structure and is likely the cause of nonproductive infections.

EXPERIMENTAL PROCEDURES

Chemicals. All reagents were of analytical grade. Distilled water was filtered and deionized through a Millipore water purification system. The experiments were performed at 20 °C in the standard buffer: 10 mM Tris, pH 7.5. Ultrapure urea was obtained from Sigma Chemical Co.

Virus Preparation. VSV type Indiana was grown on BHK-21 cells (*27*) in Dulbecco's modified Eagle's medium (DMEM) supplemented with 5% fetal bovine serum, 0.4% vitamins, and 1% nonessential amino acids and buffered with sodium bicarbonate. Purified viruses were prepared as described before (*22*).

Preparation of Glycoprotein. G protein purification was carried out as described before (*28*) with the necessary adaptations. Purified viruses were diluted in 10 mM Tris (pH = 7.5) containing the detergent octyl β-D-glucoside (Sigma Chemical Co.) in a ratio to give a final concentration of 30 mM octyl glucoside and 1 mg/mL virus protein. The suspension was allowed to stand at room temperature for 1 h. Virus nucleocapsids were pelleted by centrifugation at 35000 rpm in a Beckman SW40ti rotor for 90 min at 4 °C. The supernatant was placed in a 15−30% sucrose gradient containing 10 mM Tris (pH = 7.5), 500 mM NaCl, and 60 mM octyl glucoside and centrifuged at 38000 rpm in a Beckman SW40ti rotor for 20 h at 4 °C. The gradient was collected in fractions of 500 μL, and the absorbance was measured at 280 nm. The peak fractions were subjected to sodium dodecyl sulfate−polyacrylamide gel electrophoresis in the presence of denaturant agents to test for purity. The samples were then pooled and dialyzed against 4 L of deionized distilled water.

Virus Labeling and Fluorescence Microscopy. Virus samples were labeled with fluorescein isothiocyanate (FITC) (Molecular Probes Inc.), and cells infected with the labeled virus were observed in a fluorescence microscope as described previously (*14*).

Liposome Preparation. 1,2-Dipalmitoyl-2-oleyl-*sn*-glycero-3-phosphocholine (DOPC), 1,2-dipalmitoyl-*sn*-glycero-3-phospho-L-serine (sodium salt) (DPPS), *N*-(7-nitro-2,1,3-benzoxadiazol-4-yl)phosphatidylethanolamine (*N*-NBD-PE), and *N*-(lissamine rhodamine B sulfonyl)dihexadecanoyl-*sn*-glycero-3-phosphatidylethanolamine (*N*-RH-PE) were obtained from Avanti Polar Lipids. Lipids were diluted and mixed in chloroform, and the lipid mixture was dried under a nitrogen stream. Lipid films were then hydrated in Tris−MES buffer (30 mM Tris, 20 mM MES), pH 7.5 for pressure-induced or pH 6.0 for acid-induced fusion assay. Unilamelar vesicles were prepared by extrusion through polycarbonate membrane filters with a pore size of 0.1 μm. Unlabeled liposomes were composed of DOPC:DPPS (1:1 molar ratio), and labeled liposomes were composed of DOPC:DPPS:*N*-NBD-PE:*N*-RH-PE at a percent molar ratio of 49.4:49.4:0.6:0.6.

Fusion Assay. Membrane fusion activity was monitored by using a fluorescence resonance energy transfer (FRET) assay. Fusion was detected as the decrease in rhodamine fluorescence emission intensity. Fluorescence was monitored in a thermostated cuvette holder with excitation at 460 nm and emission at 590 nm and continuous stirring. The lipid mixing end point is defined as the fluorescence decrease observed at 590 nm on addition of Triton X-100 to 1%. The fusion extension was calculated as a fraction of the total lipid mixing (fluorescence decrease observed for the sample divided by the total decrease observed in 1% of Triton X-100) for each sample. Fusion was triggered by adding the virus samples to suspensions of mixed labeled and unlabeled liposomes (1:1) at different pHs.

Fluorescence Spectroscopy and High-Pressure Measurements. Fluorescence spectra were recorded on ISSPC or ISSK2 spectrofluorometers (ISS Inc., Champaign, IL). The high-pressure cell (*29*) was purchased from ISS Inc. (Champaign, IL). The tryptophan residues were excited at 280 nm, and emission was observed from 305 to 420 nm. Changes in fluorescence spectra at pressure p were evaluated by the changes in the spectral center of mass, $\langle \upsilon_p \rangle$:

$$\langle \upsilon_p \rangle = \sum \upsilon_i F_i / \sum F_i \qquad (1)$$

where F_i stands for the fluorescence emitted at wavenumber υ_i and the summation is carried out over the range of appreciable values of F.

The samples were allowed to equilibrate for 15 min prior to measurements being made (high-pressure and urea experiments). This time was chosen because the spectroscopic changes reached a plateau within the first 10 min and did not change significantly during longer times (several hours). Bis-ANS was excited at 360 nm and the emission collected from 400 to 600 nm. Changes were evaluated by changes in spectral area or in spectral center of mass as described above. Concentrations of the probe are as described in the figure legends. Unless otherwise noted, experiments were performed at 20 °C in 10 mM Tris, pH 7.5.

Light Scattering. Light scattering was measured in an ISSPC spectrofluorometer (*30*). Scattered light (320 nm) was collected at an angle of 90° to the incident light.

RESULTS

Pressure Converts VSV Particles into the Fusogenic State As Measured by Fusion with Cells and Liposomes. In Figure

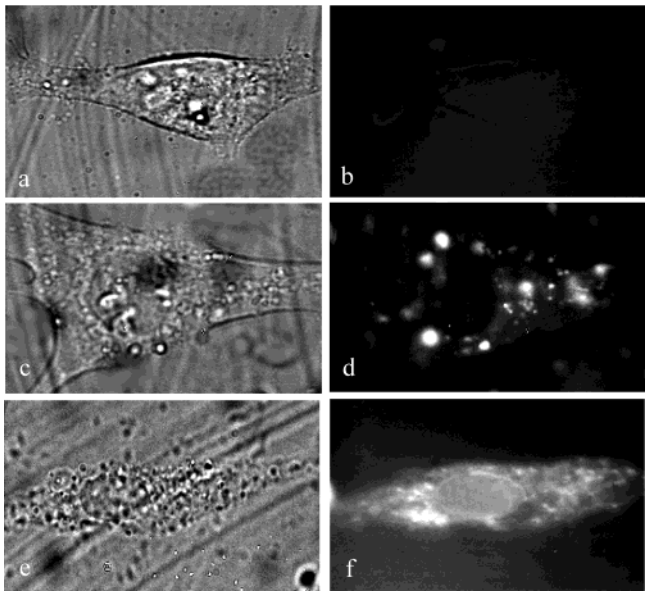

FIGURE 1: Endocytosis of native VSV vs fusion of pressure-inactivated particles. BHK-21 cells were incubated with FITC-labeled VSV particles for 30 min. Phase contrast images of cells are in panels a, c, and e. FITC fluorescence images are in panels b, d, and f. (a, b) Cells infected with nonlabeled nonpressurized particles did not show FITC fluorescence. (c, d) Fluorescence of nonpressurized labeled virus is localized in cytoplasmic vesicles. (e, f) Fluorescence of pressure-inactivated, labeled particles is dispersed in the cell.

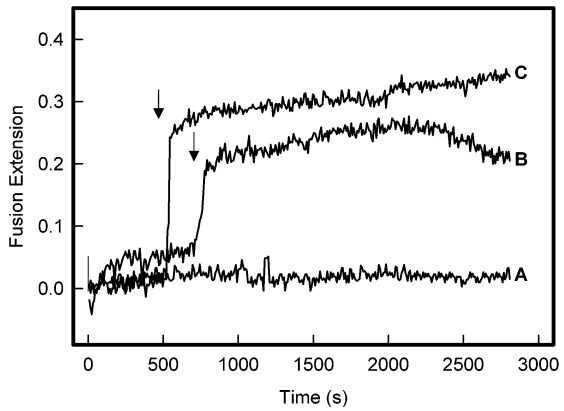

FIGURE 2: Fusion of VSV particles to liposomes induced by pressure or acidic pH. Fusion activities of different samples of VSV were measured by means of lipid mixing between labeled and unlabeled liposomes. Suspensions of labeled and unlabeled liposomes were prepared at a ratio of 1:1, and fusion was triggered by adding the virus samples. (A) Native VSV does not induce fusion at pH 7.5. (B) Acid-induced activity was measured by adding the native virus sample to the lipid suspension preincubated at pH 6.0. (C) Virus samples were pressurized at 3.1 kbar for 4 h at pH 7.5; after pressure release the samples were added to a cuvette containing the lipid suspension at pH 7.5. The final protein concentration was 0.85 mg/mL. All curves were obtained at 37 °C. The arrows indicate the moment of virus sample addition.

1, we used a previously developed method to directly visualize the early events of VSV viral infection by selective fluorescence labeling of the G protein (*14*). A pressure of 3.0 kbar reduces VSV infectivity by more than 5 orders of magnitude (*22*). After 3 h at 2.5 kbar, FITC-labeled VSV was completely inactivated (infectivity titer reduced to zero). While fluorescence of nonpressurized labeled virus enters the cell by endocytosis (Figure 1c,d), cells incubated with the virus primed to fusion by pressure displayed G protein fluorescence widely dispersed over the cell profile with almost no localized high-intensity spots (Figure 1e,f). This is consistent with fusion to the surface membrane. Our results suggest that VSV particles treated with pressure become inactive but have a propensity to fuse with cell membranes. Accordingly, although pressure induces a fusogenic state, it inactivates the particle, preventing internalization by endocytosis. The attachment of inactivated VSV to the cell without eliciting infection may be crucial to evoke a strong immune response, which is particularly relevant for the use of hydrostatic pressure as a tool to produce antiviral vaccines (*22*, *24*, *25*, *38*).

The fluorescence microscopy studies indicate that pressure incubation of VSV leads to irreversible conformational changes in the G protein that are probably similar to those promoted by low pHs. To evaluate quantitatively the changes produced by high pressure into a fusion-active state, measurements of lipid mixing between VSV virus particles and liposomes were performed (Figure 2). Lipid vesicles were prepared with two incorporated fluorescent lipid derivatives, *N*-NBD-PE (fluorescence donor) and *N*-Rh-PE (fluorescence acceptor), as described in earlier studies (*26*). Because the efficiency of energy transfer is dependent on the surface densities of fluorophores in membranes, when the fusion event takes place, and mixing between labeled and unlabeled lipids happens, the density of fluorophores decreases, causing a decrease in transfer efficiency. Thus a decrease of the fluorescence intensity of the acceptor can be used to monitor the fusion process. Figure 2 shows that high-pressure treatment (trace C) is equally efficient to elicit fusion as the decrease in pH (trace B).

Binding of Bis-ANS Reveals the Conversion of VSV into the Fusogenic State. Bis-ANS is a fluorescent probe that binds noncovalently to hydrophobic segments of protein molecules. Binding of bis-ANS to these hydrophobic pockets causes an increase in the fluorescence quantum yield of the probe. This characteristic has been used to observe protein structural changes (*22*, *31*−*33*). Bis-ANS has also been used to follow changes in the conformation of an enveloped virus as it assumes the fusion-active state (*26*, *34*, *35*).

As bis-ANS binds to protein, one can observe an increase in the fluorescence emission intensity of the probe as well as a blue shift of the emission energy. To study the binding of bis-ANS to VSV glycoprotein, a highly purified G protein was obtained as described in Experimental Procedures (Figure 3A). The purity of the purified proteins was assessed by gradient SDS−PAGE from 7% to 15% in the presence of denaturant agents (inset of Figure 3). The isolated G protein binds bis-ANS with high affinity, and the titration curve levels off at about 2 μM (Figure 3A).

Because bis-ANS binding to VSV particles occurs mostly in the G protein, it could be used to evaluate the changes into a fusogenic state of the G protein in the VSV particle (Figure 3B). The correlation between the fusogenic state and binding of bis-ANS has been established for influenza virus (*34*, *35*) and HIV (*36*). Similarly to influenza virus, the fusogenic state of VSV triggered by pH undergoes a significant increase in the fluorescence of bis-ANS (Figure 3B). We used low pH as a general destabilizing agent associated with pressure with the aim to compare the conformational changes promoted by both pressure and low

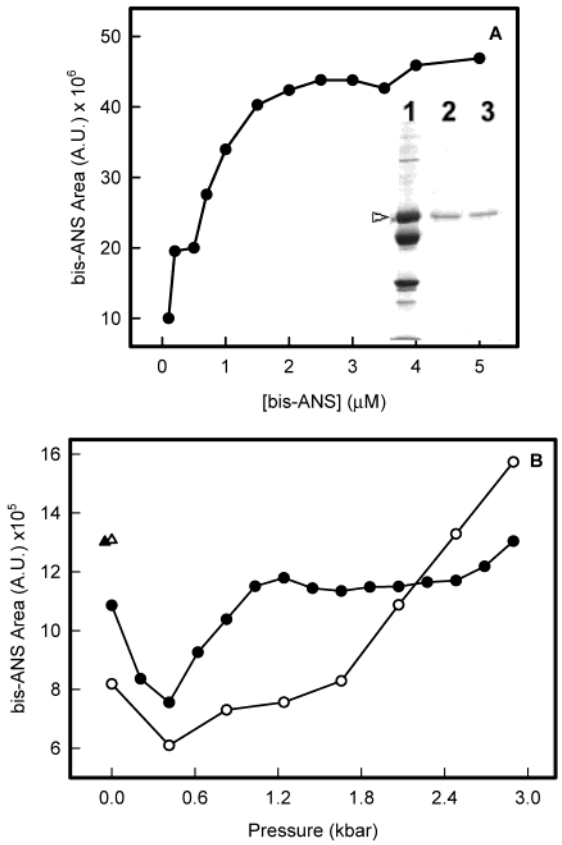

FIGURE 3: Pressure-induced enhancement of bis-ANS fluorescence bound to purified G protein and to whole VSV particles at neutral and low pH. (A) Purified G protein was incubated at different concentrations of bis-ANS and the total fluorescence measured. The fluorescence of bis-ANS in the absence of protein was subtracted from the fluorescence of bis-ANS in the presence of G protein. The excitation wavelength was 360 nm and the emission range 400−600 nm. Other experimental conditions are as described under Experimental Procedures. (Inset) Purified G protein samples were analyzed by gradient polyacrylamide gel electrophoresis from 7% to 15% under denaturant conditions: VSV particles (lane 1); fractions of two different sucrose gradients containing purified G protein (lanes 2 and 3). The arrowhead indicates the position of the G protein band. (B) VSV suspensions were diluted in 10 mM Tris buffer, pH 7.5 (open circles), or in 10 mM Bis-Tris buffer, pH 6.0 (closed cicles), to a final concentration of 100 μg/mL. In both samples the bis-ANS concentration was 2 μM. Open and closed triangles at the left represent the value of bis-ANS fluorescence after decompression for the samples at pH 7.5 and 6.0, respectively. Data points represent the average of three measurements, and the standard deviation was within the size of the symbol.

pH (Figure 3B). During the viral infection cycle the acid pH is crucial to elicit infection (*2*). VSV entire particles were incubated in neutral (Figure 3B, open circles) or acid pH (Figure 3B, filled circles), and bis-ANS fluorescence was measured. Samples were then subjected to increasing hydrostatic pressure. The initial points in the curve show that VSV incubated in low pH binds more bis-ANS at atmospheric pressure than the samples in pH 7.5. This is in agreement with the uncovering of hydrophobic segments induced by low pH. Bis-ANS binding increases gradually at pH 7.5 as pressure increases, whereas at pH 6.0 a slight change was observed. Pressure effects were partially irreversible. When pressure was released, values of bis-ANS fluorescence changed to the same value for both samples (triangles), this value being different from the initial point

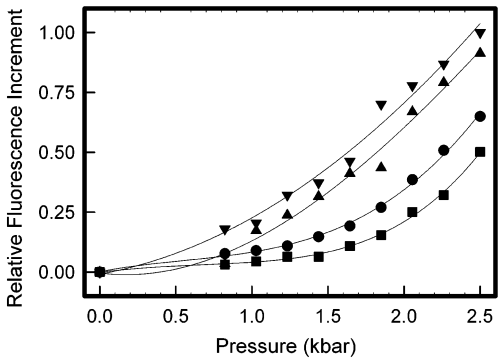

FIGURE 4: Changes in bis-ANS fluorescence bound to VSV as a function of pressure and subdenaturing urea concentrations. VSV suspensions of 50 μg/mL and 2 μM bis-ANS incubated with the following: no urea (circles); 0.5 M urea (squares); 1 M urea (triangles); 2 M urea (inverted triangles). The excitation wavelength was 360 nm. The collected emission was 400−600 nm. The intensity at each pressure (I) was normalized to the value at atmospheric pressure (I_0).

(Figure 3B). The small decrease observed in the initial points can be explained by the effects of pressure on some less specific sites in the glycoprotein or in the membrane, which are also sensitive to pressure.

Conformational changes caused by urea and pressure are different, but the concomitant utilization of subdenaturing urea concentrations and pressure can give insight into protein stability studies (*37*). VSV suspensions were subjected to pressure in the presence of urea (Figure 4). Bis-ANS binding was observed for different urea concentrations (0−2 M). Pressure alone caused conformational changes observed as an increase in bis-ANS fluorescence. As the concentration of urea is increased, lower pressures are needed to promote the increase in bis-ANS binding. Samples pressurized in the presence of urea presented more relative increase in bis-ANS fluorescence than the samples pressurized without urea, confirming that urea has magnified the effects of pressure. Urea has been previously used to attain the fusogenic state of influenza viruses (*2*). Our results indicate that the fusogenic state of VSV is triggered by pressure and that it involves exposure of hydrophobic domains. Similar to influenza viruses (*2*), urea appears to cooperate to attain the fusion-active state.

Comparison of Pressure Stability of G Protein and VSV. Previous studies have shown that pressure causes changes to VSV particles leading to inactivation (*22*, *31*). Figure 5 shows the comparison of pressure stability of VSV entire particles and isolated G protein. Both samples were subjected to increasing values of pressure up to 2.9 kbar. The changes were followed by tryptophan emission fluorescence as observed by the changes in average energy of the emission (the spectral center of mass in wavenumbers). Considering the content of tryptophans of all the different viral proteins (*39*−*41*), VSV entire particles contain approximately 33913 tryptophans. Since each G protein contains 13 tryptophans and there are approximately 1205 molecules of G protein/particle, the tryptophans in G proteins account for 47% of the total. A similar relation exists for the tyrosines. Thus, about 50% of the intrinsic fluorescence of whole VSV particles comes from the G protein. VSV entire particles (squares) and isolated G protein samples (circles) show similar changes under pressure treatment. The results in

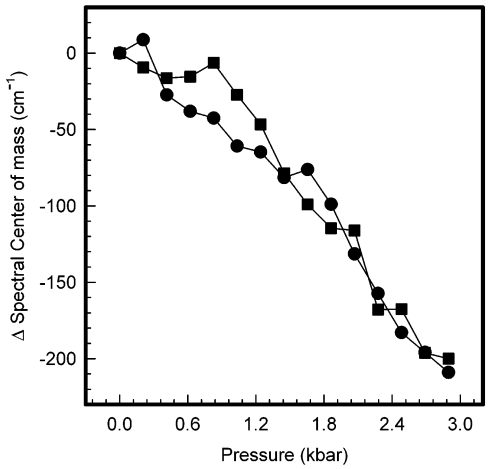

FIGURE 5: Comparison of pressure stability of G protein and VSV. Isolated G protein samples (circles) and VSV entire particles (squares) were subjected to different pressure values as shown on the abscissa. Similar changes in the spectral center of mass of both were observed during pressurization up to 2.9 kbar.

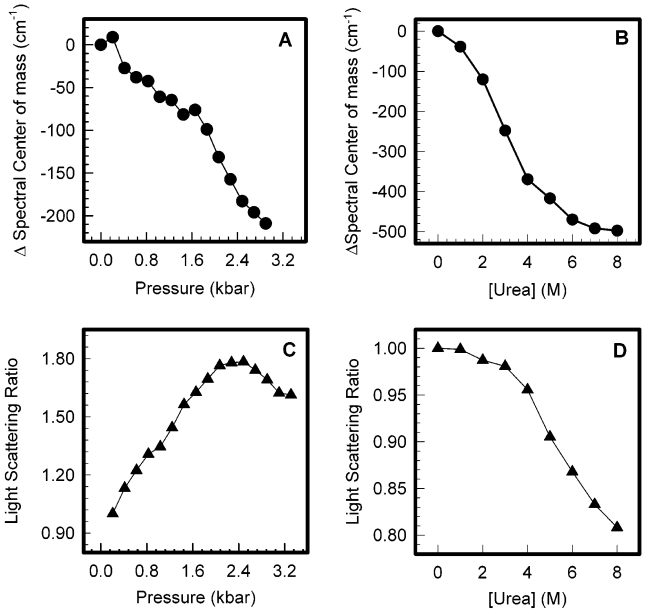

FIGURE 6: Stability of G protein against pressure and urea. Purified G protein samples were diluted in 10 mM Tris buffer at pH 7.5 to a final concentration of 100 μg/mL. The fluorescence excitation wavelength was 280 nm, and the emission wavelength range was 305−420 nm. Changes in tryptophan fluorescence emission spectra were observed during the pressurization process up to 3.1 kbar (A) and with the increase in urea concentration (B). (C) Increase in light scattering values as a function of pressure and (D) decrease in light scattering values by urea treatment. For light scattering, the samples were excited at 320 nm, and scattered light was measured at the same wavelength. Data points represent the average of three independent measurements.

Figure 5 demonstrate that pressure-induced inactivation of VSV is due to changes caused on the G protein spikes that protrude through the virus envelope.

Pressure and Urea Stability of G Protein. The stability of VSV glycoprotein under urea and pressure treatment was tested. Figure 6 shows the changes in G protein tryptophan fluorescence emission by means of the spectral center of mass. Pressure caused only a partial conformational change (Figure 6A) while the urea treatment promoted total denaturation of the protein (Figure 6B). Light scattering measurements were used to assess information on the size of the particles present in the suspension. There was an increase in light scattering caused by increasing pressure (Figure 6C), suggesting that high pressure promoted more interactions between G protein molecules. A decrease in light scattering was observed with the increase of the urea concentration (Figure 6D). These results strongly suggest that pressure causes much less change in the tertiary structure of the G protein than urea.

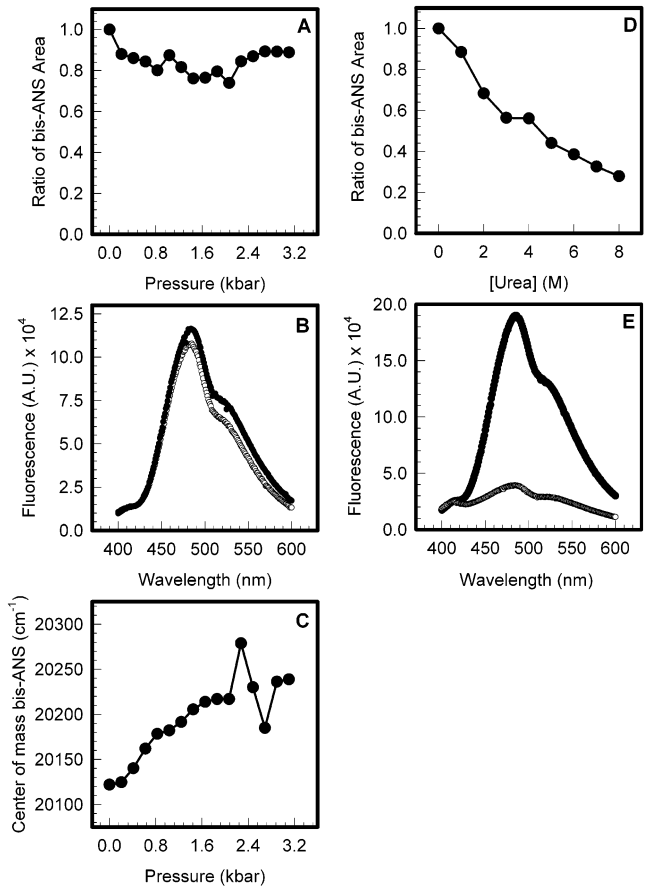

FIGURE 7: Bis-ANS binding to native G protein. Purified G protein samples were incubated with 3 μM bis-ANS and subjected to high pressure (A) or incubated with increasing urea concentrations (D). (B) Bis-ANS fluorescence emission spectra at atmospheric pressure (open circles) and at 3.1 kbar (closed circles). (C) Changes on the spectral center of mass of bis-ANS as a function of pressure. (E) Bis-ANS fluorescence emission spectra in the absence of urea (closed circles) and in the presence of 8 M urea (open circles).

We also compared the changes in secondary structure of the G protein produced by pressure and urea. The circular dichroism at 222 nm was less than 5% changed after pressure treatment, whereas low pH reduced the ellipticity by 52% and 8 M urea reduced it to almost zero. It can be concluded that pressure causes little or no change in secondary structure in contrast to urea that causes complete unfolding of the G protein.

Hydrophobic Exposure of the G Protein As It Is Converted into the Fusogenic State. To evaluate the nature of the conformational changes in the G protein, purified samples were incubated with bis-ANS and subjected to pressure or urea treatment (Figure 7). Increasing pressure did not cause a significant change in the fluorescence intensity, but a blue shift of the emission could be observed in Figure 7B and titrated by the changes in the energy of emission (Figure 7C), indicating binding of the probe to hydrophobic sites.

High urea concentrations completely eliminated bis-ANS binding (Figure 7D,E). The increase in the average wavenumber of bis-ANS fluorescence observed during the high-pressure treatment indicates partition into more hydrophobic segments as pressure increases (Figure 7C).

The exposure of hydrophobic segments could be responsible for promoting more protein−protein interactions as observed in Figure 6 with the increase of light scattering as a function of pressure. The fact that high urea concentration abolishes bis-ANS binding is in agreement with the drastic conformational changes in fluorescence, light scattering (Figure 6), and circular dichroism. The lack of bis-ANS binding is characteristic of the absence of structure, confirming the complete denaturation of G protein by high urea concentrations.

DISCUSSION

The VSV glycoprotein is the protein responsible for cell receptor recognition and membrane fusion. The acid pH in the endosome is required for the protein to trigger its fusogenic activity (*2*, *5*, *6*, *9*, *42*). We investigated the effects of high hydrostatic pressure and urea on the VSV G protein to understand the conformational changes involved in its fusogenic activity. Here we show that hydrostatic pressure switches the VSV G protein into the fusogenic state. The pressure-induced fusion of VSV with liposomes was of equal magnitude to that triggered by low pH (Figure 2).

Previously, we have shown that both influenza and Sindbis viruses are inactivated by pressure with the main change occurring in the envelope protein that undergoes a transition to the fusogenic state (*26*). This is in agreement with the metastability model proposed to fusion proteins of enveloped viruses (*2*). Meanwhile, irreversibility is a prerequisite for metastability, and this is not the case for rhabdoviruses. It has been shown that Rhabdovirus family G proteins undergo a reversible conformational change to the fusogenic state triggered by low pH (*6*, *9*, *43*). In our studies, we have shown that the conformational changes caused by pressure are partially irreversible at either pH 7.5 or pH 6.0 (Figure 3B). However, the profiles presented by the curves in Figure 3B suggest different ways to reach the same final conformation observed after pressure release. Gaudin et al. (*43*) have shown by monoclonal antibody recognition and sensitivity to proteases that three different conformations of rabies virus G protein can be induced by the different pHs: (1) one nonfusogenic native state at pH 7.4, (2) a second conformation that tightly binds to membranes but is still nonfusogenic at pH 6.4, and (3) a third one at pH 5.9 that promotes membrane fusion and virus particle aggregation (*43*). All of these conformational changes could be reverted on reneutralization except for the virus aggregation at pH 5.9. Pak et al. (*9*) proposed that VSV G undergoes a proton-driven shift from the native T (tense) state at neutral pH either to a fusion-active R (relaxed) state or to a fusion-inactive D (desensitized) state. They also showed that the conformational changes are followed by insertion of the fusion-active region of the protein into the target membrane (R state) or not (D state) (*44*).

Our results show that a compression−decompression cycle promoted the same global conformational change on both low and neutral pH forms of VSV G protein (Figure 3B). This suggests that pressure is populating a common intermediate state from which the final conformation is reached.

Fluorescence, light scattering, and circular dichroim showed that urea promoted complete unfolding of the protein whereas pressure promoted only a partial conformational change (Figure 6). The bis-ANS binding assays show that this probe binds to the native protein and that the conformational change promoted by pressure leads to the uncovering of hydrophobic segments, as indicated by the increase in the spectral center of mass of bis-ANS (Figure 7C) and bis-ANS spectral area (Figures 3 and 4). These results also indicate the presence of hydrophobic cavities in the protein. High urea concentrations completely eliminated the bis-ANS binding (Figure 7D,E), confirming the protein denaturation and the different nature of the changes caused by urea and pressure.

Pressure provokes inactivation of VSV particles (*22*). The changes caused by pressure on VSV particles and isolated G protein samples are very similar, suggesting that the virus inactivation caused by pressure is due to changes on the G protein (Figure 5). G proteins appear to undergo aggregation at pH 5.9 in the absence of a target membrane (*43*) likely because of the exposure of hydrophobic regions. We do find that pressure promotes protein−protein interactions as observed by the increase in light scattering of purified G protein (Figure 6C). Hydrostatic pressure can either induce or prevent protein aggregation (*45*−*47*). The uncovering of hydrophobic segments in viral particles caused by pressure resembles the low-pH effect (Figures 3, 4, and 7C). Gaudin et al. (*43*) observed morphological changes of rabies particles when they were aggregated at pH 5.9. Morphological changes of VSV were also observed after pressure inactivation (*22*).

Pressure-induced conformation is not the desensitized state since it binds to the membrane of target cells (Figures 1 and 2), and the described D state did not show interaction with target membranes (*9*). Pressure affects mainly hydrophobic interactions, especially by inducing the penetration of water molecules into protein structures (*48*−*50*). It is likely that pressure-induced fusogenic conformation is the result of pressure effects on the hydrophobic interactions of G proteins, mimicking the change of protein−protein interactions for protein−target membrane interactions. As this happens in the absence of the target membrane, this final conformation resembles the pH-induced fusogenic conformation. The irreversibility of the pressure effects (Figure 3) may also have the contribution of the effects on the protein−lipid and protein−protein interactions, such as in the contacts between the G and M proteins in the VSV particle.

High pressure was used in this study to characterize pressure-induced conformational changes that lead to the fusogenic state, similar to that characterized at acid pH (*2*, *6*, *9*, *43*, *44*). As the changes caused by pressure were partially irreversible, we strongly propose that pressure is inducing a fusion-intermediate state of the G protein, which gives rise to the loss of infectivity and causes nonproductive infections.

ACKNOWLEDGMENT

We are grateful to Emerson R. Gonçalves for competent technical assistance.

REFERENCES

1. Weissenhorn, W., Dessen, A., Calder, L. J., Harrison, S. C., Skehel, J. J., and Wiley, D. C. (1999) *Mol. Membr. Biol. 16*, 3−9.
2. Carr, C. M., Chaudhry, C., and Kim, P. S. (1997) *Proc. Natl. Acad. Sci. U.S.A. 94*, 14306−14313.
3. Mayer, A. (2001) *Trends Biochem. Sci. 26*, 717−723.
4. Skehel, J. J., and Wiley, D. C. (1998) *Cell 95*, 871−874.
5. Schlegel, R., Willingham, M. C., and Pastan, I. H. (1982) *J. Virol. 43*, 871−875.
6. Blumenthal, R., Bali-Puri, A., Walter, A., Covell, D., and Eidelman, O. (1987*) J. Biol. Chem 262*, 13614−13619.
7. Crimmins, D. L., Mehard, W. B., and Schlesinger, S. (1983) *Biochemistry 22*, 5790−5796.
8. Thomas, D., Newcomb, W. W., Brown, J. C., Wall, J. S., Hainfeld, J. F., Trus, B. L., and Steven, A. C. (1985) *J. Virol. 54*, 598−607.
9. Pak, C. C., Puri, A., and Blumenthal, R. (1997) *Biochemistry 36*, 8890−8896.
10. Clague, M. J., Schoch, C., Zech, L., and Blumenthal, R. (1990) *Biochemistry 29*, 1303−1308.
11. Wagner, R. R. (1987) in *The Rhabdoviruses* (Wagner, R. R., Ed.) pp 9−74, Plenum Press, New York.
12. Weck, P. K., and Wagner, R. R. (1978) *J. Virol. 25*, 770−780.
13. McGowan, J. J., and Wagner, R. R (1981) *J. Virol. 38*, 256−257.
14. DaPoian, A. T., Gomes, A. M. O., Oliveira, R. J. N., and Silva, J. L. (1996) *Proc. Natl. Acad. Sci. U.S.A. 93*, 8268−8273
15. Silva, J. L., and Weber, G. (1993) *Annu. Rev. Phys. Chem. 44*, 89−113.
16. Mozhaev, V. V., Heremans, K., Frank, J., Masson, P., and Balny, C. (1996) *Proteins 24*, 81−91.
17. Silva, J. L., Foguel, D., and Royer, C. R. (2001) *Trends Biochem. Sci. 26*, 612−618.
18. De Sousa, P. C., Jr., Tuma, R., Prevelige, P. E., Jr., Silva, J. L., and Foguel, D. (1999) *J. Mol. Biol. 287*, 527−538.
19. Leimkuhler, M., Goldbeck, A., Lechner, M. D., and Witz, J. (2000) *J. Mol. Biol. 296*, 1295−1305.
20. Leimkuhler, M., Goldbeck, A., Lechner, M. D., Adrian, M., Michels, B., and Witz, J. (2001) *Arch. Virol. 146*, 653−667.
21. Oliveira, A. C., Gomes, A. M. O., Almeida, F. C. L., Mohana-Borges, R., Valente, A. P., Reddy, V. S., Johnson, J. E., and Silva, J. L. (2000) *J. Biol. Chem. 275*, 16037−16043.
22. Silva, J. L., Luan, P., Glaser, M., Voss, E. W., and Weber, G. (1992) *J. Virol. 66*, 2111−2117.
23. Oliveira, A. C., Ishimaru, D., Gonçalves, R. B., Mason, P., Sá-Carvalho, D., Smith, T. J., and Silva, J. L. (1999) *Biophys. J. 76*, 1270−1279.
24. Tian, S. M., Ruan, K. C., Qian, J. F., Shao, G. Q., and Balny, C. (2000) *Eur. J. Biochem. 267*, 4486-4494.
25. Pontes, L., Cordeiro, Y., Giongo, V., Villas-Boas, M., Barreto, A., Araújo, J. R., and Silva, J. L. (2001) *J. Mol. Biol. 307*, 1171−1179.
26. Gaspar, L. P., Silva, A. C., Gomes, A. M., Freitas, M. S., Ano Bom, A. P., Schwarcz, W. D., Mestecky, J., Novak, M. J., Foguel, D., and Silva, J. L. (2002) *J. Biol. Chem. 277*, 8433−8439.
27. Cartwright, B., Smale, C. J., and Brown, F. (1969) *J. Gen. Virol. 5*, 1−10.
28. Mahtieu, M. E., Grigera, P. R., Helenius, A., and Wagner, R. R. (1996) *Biochemistry 35*, 4084−4093.
29. Paladini, A. A., and Weber, G. (1981) *Rev. Sci. Instrum. 52*, 419−427.
30. Silva, J. L., Villas-Boas, M., Bonafe, C. F. S, and Meirelles, N. C. (1989) *J. Biol. Chem. 264*, 15863−15868.
31. Bonafe, C. F., Glaser, M., Voss, E. W., Weber, G., and Silva, J. L. (2000) *Biochem. Biophys. Res. Commun. 275*, 955−961.
32. Rosen, C. G., and Weber, G. (1969) *Biochemistry 8*, 3915−3920.
33. Horowitz, P., Prasad, V., and Luduena, R. F. (1984) *J. Biol. Chem. 259*, 14647−14650.
34. Korte, T., and Herrmann, A. (1994) *Eur. Biophys. J. 23*, 105−113.
35. Korte, T., Ludwig, K., Booy, F. P., Blumenthal, R., and Herrmann, A. (1999) *J. Virol. 73*, 4567−4574.
36. Jones, P. L., Korte, T., and Blumenthal, R. (1998) *J. Biol Chem. 273*, 404−409.
37. Weber, G., Da Poian, A. T., and Silva, J. L. (1996) *Biophys. J. 70*, 167−173.
38. Jurkiewicz, E., Villas Boas, M., Silva, J. L., Weber, G., Hunsmamm, G., and Clegg, R. M. (1995) *Proc. Natl. Acad. Sci. U.S.A. 92*, 6935−6937.
39. Schubert, M., Harmison, G. G., and Meier, E. (1984) *J. Virol. 51*, 505−514.
40. Gallione, C. J., Greene, J. R., Iverson, L. E., and Rose, J. K. (1981) *J. Virol. 39*, 529−535.
41. Rose, J. K., and Gallione, C. J. (1981) *J. Virol. 39*, 519−528.
42. Matlin, K. S., Reggio, H., Helenius, H., and Simons, K. (1982) *J. Mol. Biol. 156*, 609−631.
43. Gaudin, Y., Tuffereau, C., Segretain, D., Knossow, M., and Flamand, A. (1991) *J. Virol. 65*, 4853−4859.
44. Puri, A., Grimaldi, S., and Blumenthal, R. (1992) *Biochemistry 31*, 10108−10101.
45. Gorovits, B. M., and Horowitz, P. M. (1998) *Biochemistry 37*, 6132−6135.
46. Smeller, L, Rubens, P., and Heremans, K. (1999) *Biochemistry 38*, 3816−3820.
47. Ferrão-Gonzales, A. D., Souto, S. O., Silva, J. L., and Foguel, D. (2000) *Proc. Natl. Acad. Sci. U.S.A. 97*, 6445−6450.
48. Oliveira, A. C., Gaspar, L. P., Da Poian, A. T., and Silva, J. L. (1994) *J. Mol. Biol. 240*, 184−187.
49. Hummer, G., Garde, S., García, A. E., Paulaitis, M. E., and Pratt, L. R. (1998) *Proc. Natl. Acad. Sci. U.S.A. 95*, 1552−1555.
50. Silva, J. L., Oliveira, A. C., Gomes, A. M. O., Lima, L. M., Mohana-Borges, R., Pacheco, A. B. F., and Foguel, D. (2002) *Biochim. Biophys. Acta 1595*, 250−265.

BI027207K